Nacre Paper

DOI: 10.1002/anie.201001577

Supramolecular Control of Stiffness and Strength in Lightweight High-Performance Nacre-Mimetic Paper with Fire-Shielding Properties**

Andreas Walther, Ingela Bjurhager, Jani-Markus Malho, Janne Ruokolainen, Lars Berglund, and Olli Ikkala**

Biological materials fascinate us with their ability to withstand extreme mechanical forces under complex conditions. Their excellent performance originates from a multilevel hierarchical structure; understanding these structures is pursued in structural biology and biomechanics research. A common feature in many biological materials with superior mechanical properties is the combination and ordered arrangement of hard and soft building blocks.[1–3] Therein, the hard matter serves as the load bearing and reinforcing part, whereas energy can be dissipated into the soft segments. Many of these materials combine good toughness with admirable strength and stiffness. For instance, in nacre, the layered arrangement of platelet-shaped $CaCO_3$ crystals and proteins into a brick and mortar structure leads to a synergistic performance with respect to the mechanical properties.[5] The Young's modulus and stress at break can reach 40–70 GPa and 80–135 MPa, respectively.[6–8] The material is remarkably tough under wet conditions. Dynamic processes, such as sacrificial (dynamic) bonds and hidden length scales contribute significantly to toughness improvements or the ability of a material to undergo self-healing. Recently, it was shown that infiltration of metal ions drastically increase the toughness of silk dragline or increase stiffness and strength in layer-by-layer (LbL) materials.[9,10] Moreover, modeling by Fratzl and co-workers showed how randomly distributed multivalent binding sites in layered materials can lead to sacrificial bonds and provide shear deformability and larger deformations similar to that found in natural materials.[12] Thus, ionic bonding is a promising tool for tailoring the mechanical properties of biological or biomimetic systems, and to access important features such as sacrificial bonds and hidden length scales.

Considering the lightweight character of the mechanically strong and tough biomaterials, a large-scale preparation of biomimetic materials is of preeminent importance for future construction and coating applications. However, this is a major scientific challenge. Various efforts have been undertaken to mimic the layered hard/soft composite structure of nacre by synthetic means. Nacre mimics can be obtained by several sequential approaches, such as layer-by-layer (LbL)[13–16] and other multilayer deposition strategies,[17] ice-templating and sintering of ceramics,[18,19] uncontrolled co-casting of polymer/clay mixtures,[20–22] or processes at interfaces.[23–25] Unfortunately, most of the approaches are limited to the structural characterization of the materials at very small scales, and often there have been challenges in even producing large enough specimens for mechanical characterization beyond nanointendation. Using LbL[26] deposition of polymers and nanoclay, the maximum stiffness and strength could even exceed those of natural nacre,[13–16] thus demonstrating how valuable such layered polymer/clay structures can be. Toughness could be increased by repeated spin coatings of chitosan and monolayer transfer of Al_2O_3 platelets for the generation of ordered hybrid composite materials.[17] These techniques, despite yielding very interesting materials, are however very laborious and time-consuming, as they require the repeated and sequential deposition of individual layers for the build-up of multilayered structures. Even the achievement of thicknesses of several micrometers will typically take several days, and only finite-sized specimens can be addressed. Clearly, the unfortunate combination of very appealing properties and challenging production calls for conceptually novel strategies that enable for a scale-up and a continuous production.

Recently, we introduced paper-making, doctor-blading, and simple painting as methods for the simple and fast production of nacre-mimetic sub-millimeter thick films, laminates, and coatings toward specimens with potentially infinite lateral dimensions and excellent mechanical properties.[27] A key step is the fact that the generation of self-assembled hard/soft layered composites is not restricted to sequential depositions. On the contrary, we can prefabricate core/shell hard/soft building blocks on a large scale in water by borrowing concepts of colloid science. The generation of such bricks relies on the polymer coating of individual hard platelet-shaped nanoclays, montmorillonite (MTM, Na-Cloisite, thickness ca. 1 nm, diameter ca. 50–1000 nm), by polymers that specifically adsorb onto the nanoclays to form a soft layer. The completely exfoliated platelets are then forced to self-assemble on a second length by a process similar to paper-making (Scheme 1, top). Paper-making is a well-understood, robust, and up-scalable technique in which paper pulp is sucked on a filtration mat, treated with various additives, heated and pressed, and finally collected on giant rolls. The overall strategy represents most likely the fastest

[*] Dr. A. Walther, J.-M. Malho, Prof. J. Ruokolainen, Prof. O. Ikkala
Molecular Materials, Department of Applied Physics
Aalto University
00076 Aalto/Helsinki (Finland)
E-mail: andreas.walther@tkk.fi
olli.ikkala@tkk.fi
I. Bjurhager, Prof. L. Berglund
Division of Biocomposites
Royal Institute of Technology, Stockholm (Sweden)

[**] We acknowledge support by the Finnish Academy, the Wallenberg Foundation, UPM, the Nordic Hysitron Lab, and Dr. V. Aseyev.

Supporting information for this article is available on the WWW under http://dx.doi.org/10.1002/anie.201001577.

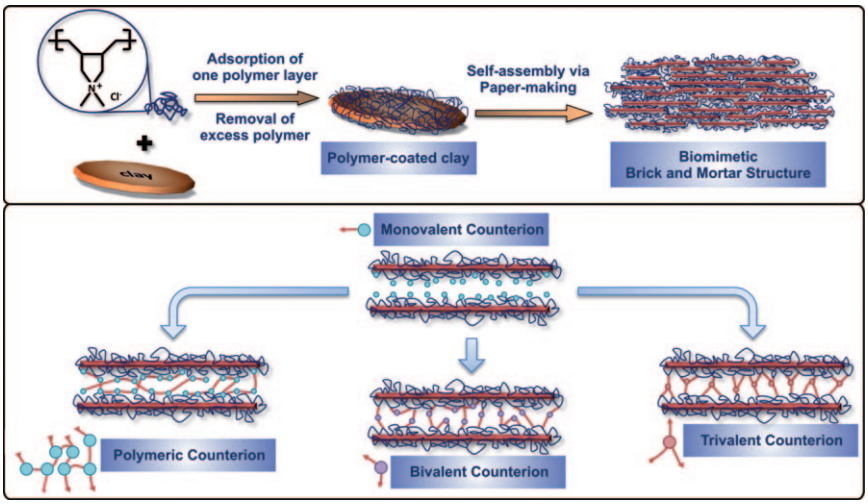

Scheme 1. Top: Multilevel self-assembly to form a nacre-mimetic brick and mortar structure by core/shell hard/soft building blocks consisting of hard inorganic MTM cores and soft polymer coatings. Bottom: Supramolecular manipulation of the interaction between the polyelectrolyte-coated clay platelets as shown for one MTM interstitial space. The amount of counterions is decreased whilst their connectivity is increased for counterions with higher valency. The polymeric counterion is shown schematically on the left.

and simplest access to nacre-mimetic thick films with excellent material properties. It is environmentally friendly and economic, and is ready for scale-up towards real applications.

The mechanical properties of such assemblies critically depend on the connectivity of the polymeric shells, as shown for the covalent cross-linking of poly(vinyl alcohol) (PVA) chains.[27] By contrast, we explore herein how ionic supramolecular bonds instead of covalent bonds can be used to tailor and strengthen the mechanical properties. Supramolecular and dynamic bonds are a key feature in biological materials, and we need to broaden our understanding in using them for synthetic biomimetic materials. Our system utilizes well-defined, single polycation-coated nanoclay platelets, as shown by a near-constant size distribution by dynamic light scattering (Supporting Information, Figure S1). We chose PDADMAC (poly(diallyldimethyl-ammonium chloride)) for its ease of availability and because we can compare our materials to previous nacre-mimetic composites obtained by sequential LbL assembly.[9,16]

Research into polyelectrolytes (PEs) has shown how counterions of different valencies, architectures, and sizes can be used to manipulate the interactions, molecular structures, and the attractions between charged macromolecules.[28–32] Scheme 1 (bottom) shows how counterions with different architectures and valencies can mediate the interactions between the polymer-coated MTM stacks and are able to strengthen the assembly. Note that our nacre-mimetic paper has more ionic groups available at the surface compared to LbL-based materials (Supporting Information, Figure S4). Thus the effect of modulating the supramolecular interactions should have a significant influence and reduce a potentially slippery interface between MTM stacks. Importantly, the internal cohesion and strength in a PE can be multiplied by increasing the valency of the counterions.

Figure 1 shows an overview of different nacre-mimetic papers. The overall thickness can easily be tailored, and so far we have usually prepared films up to a fraction of millimeters in thickness. The highly aligned self-assemblies are maintained throughout the complete sample despite the rapidness of the process. The photographs in Figure 1c,d demonstrate the high optical quality (translucency) and reasonable flexibility. The resulting structures contain a majority fraction of clay (70 wt%) as in nacre. Importantly, using LbL assembly to achieve such large thicknesses and high contents of inorganic materials would require weeks or months, whereas we can prepare those in a fraction of that

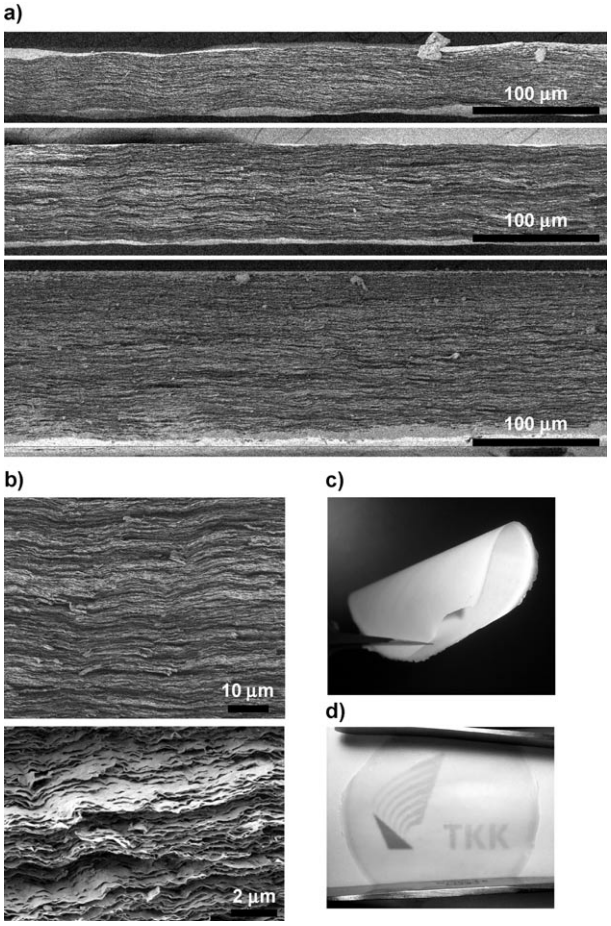

Figure 1. Various low- (a) and high-resolution (b) SEM images demonstrating the size tunability and strongly aligned layered arrangement. The photographs show good optical translucency (d) and reasonable flexibility ((c), image taken with flash) of a layered composite of 0.03 mm thickness. The picture in (d) shows the printed university logo placed behind a nacre paper.

time. The molar ratio of chlorine to nitrogen, based on elemental analysis (EA), indicates that 20–25% of the ionic groups are not bound to the clay surface and are thus available for supramolecular interaction between the nanoclays. The detailed element-sensitive mapping of the cross section by energy-dispersive X-ray (EDX) analysis shows a homogeneous distribution of the various components (Figure 2a–c). Carbon and nitrogen and also silicon and oxygen locations correspond to the locations of PDADMAC and the clay platelets, respectively. The chlorine map displays a uniform distribution of the counterions within the polymer phase. The corresponding EDX spectrum (Figure 2d) does not show any signal for sodium (the original nanoclay counterion), indicating the tight anchorage of the PDADMAC ionic groups onto the MTM.

High-resolution TEM (Figure 2e) reveals well-ordered stacks with alternating hard clay and soft polymer layers, which is further confirmed by small-angle scattering (SAXS; Supporting Information, Figure S2). Therefore, the prefabricated well-defined hard/soft bricks lead to a very regular self-assembly. In contrast, simple applications of uncontrolled and unbalanced mixtures of nanoclay and polymer without their preassembly can result in an unequal distribution of the components. The structure of the composites is thus reminiscent of nacre, albeit with a smaller thickness of the inorganic platelets.

The positively charged sites of PDADMAC having chlorine counterions are available for tailoring the supramolecular interactions between the layered polymer-coated nanoclay. Exchanging the monovalent chloride ion to bi- or trivalent ions (SO_4^{2-} or PO_4^{3-}) or creating an interpenetrating network of the counterions aimed to strengthen the cohesion between the layers and to increase the stiffness of the materials. An interpenetrating network can be created using a polymerizable counterion, such as styrene sulfonate ($StSO_3^-$), which can be thermally polymerized similarly to styrene (denoted as $(StSO_3^-)_x$).[33]

The counterion exchange can be accomplished by infiltration of the self-assembled layers of the nacre-mimetic paper. Its success can be followed by the elemental composition (EA) and mapping (EDX). After infiltration, the chloride content is strongly diminished, and new counterions can be detected (Figure 3d–f). The elemental mapping of the infiltrated counterions reveals a uniform distribution throughout the cross-section, independent of the counterion used (see Supporting Information, Figure S5 for additional EDX images). Furthermore, the EDX spectra show no indication of additional cations (Na, Cu) of the salt solutions used for the counterion exchange. Therefore, the layered composites are well-defined and free of impurity salt contaminations. Comparing the molar percentages (EA) of counterions upon exchange points to a near-quantitative replacement. The molar ratio between chlorine in the initial material and $StSO_3^-$, SO_4^{2-}, and PO_4^{3-} are 0.94, 0.54, and 0.40, and thus very near the ideal values of 1, 0.5, and 0.33, respectively. The exchange of the counterion has only a minor influence on the stacking distance of the platelets as determined by SAXS. However, the incorporation of the larger organic counterion $StSO_3^-$ leads to a slight growth of the interlayer distance. The exchange also goes along with a slight alteration of the thermal characteristics of the materials (Fiure 3a). The most pronounced increase can be seen for the organic counterion, $StSO_3^-$, which leads to slightly enhanced degradation.

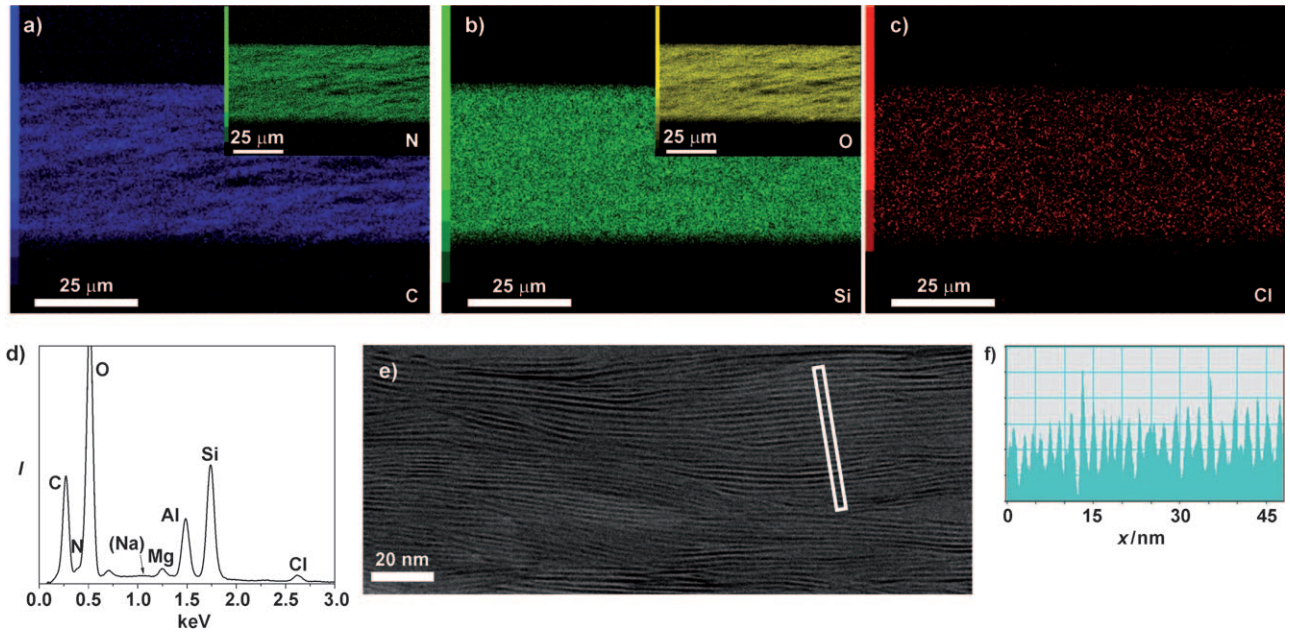

Figure 2. a–c) Energy-dispersive X-ray (EDX) mapping of the different components: a) Carbon and nitrogen (inset) for PDADMAC, b) silicon and oxygen (inset) for MTM, and c) the chloride counterion. Some darker spots are caused by the uneven cross-section of the material and the orientation of the EDX detector, which leads to some shadows, and is more pronounced for low-energy X-rays when comparing the silicon and oxygen maps originating from the MTM. d) The full EDX spectrum with the corresponding elements. The high-resolution TEM image (e) reveals an equal spacing of the MTM platelets and alternating hard and soft layers, which can also be seen from the section analysis (f).

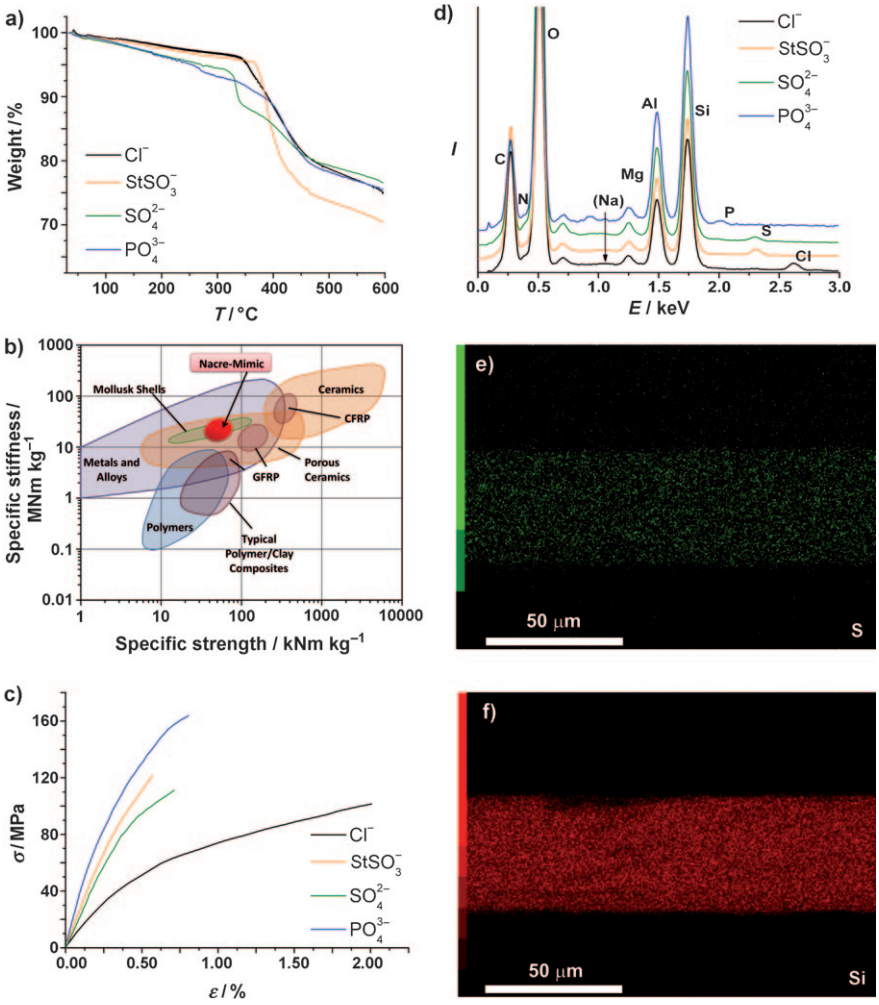

Figure 3. a) TGA analysis of the composites after counterion exchange. b) Specific materials selection chart for various materials ranked according to their density, as adapted from Ashby, Wegst, and co-workers.[4] The data for the classical polymer/clay composites was drawn based on a recent review.[11] c) Stress–strain curves (σ versus ε) obtained by tensile testing of various samples indicated in the figure. d–f) SEM-EDX elemental mapping. d) EDX traces of the various composites indicated in the figures. e,f) Elemental maps of sulfur (e) and silicon (f), showing the homogenous infiltration with counterions in the case of sulfate. (EDX maps for all samples are given in the Supporting Information, Figure S5.)

We analyzed the influence of the connectivity of the supramolecular bonding motifs on the mechanical properties by tensile testing. Table 1 and Figure 3 show the material characteristics, including their strength, stiffness, and elongation at break and the nanoclay platelet spacing. The strength and stiffness reveal excellent values. The Young's modulus approaches half of that of nacre, whilst the strength is already in the range or exceeds that of nacre.

Our composites largely outperform some of the best high-performance and yet reasonably easily processible polymers, such as polyparaphenylene or polyimide, and also traditional clay/polymer composites. The specific materials property selector chart, adapted from Reference [4], demonstrates that our nacre mimics are near the high-performance biocomposites and compete with metals, porous ceramics, and unidirectionally reinforced polymer composites.[3–5,11] All of those require sophisticated and energy-intensive preparation pathways. Turning to the detailed supramolecular tuning of the material properties, we can see that the non-modified PDADMAC(Cl)/MTM nacre mimic exhibits a stiffness of about 13 GPa and an ultimate strength of 106 MPa, which is nearly two orders of magnitude larger than the pure polymer. The stiffness in our material is almost 20% better than for the materials obtained by LbL assembly[9] ($E = 11$ GPa, $\sigma_{uts} = 100$ MPa).

A further increase in ultimate strength is prevented because brittle failure is more likely to appear in larger-scale materials. Our typical test specimens are about 50 times thicker and also somewhat longer than the minimally sized specimens previously used in LbL-based nacre mimics.[13–16] Thus we regard our tensile data to be more relevant to estimate bulk values, as our thick samples have a higher chance for cracks typically existing in bulk matter. We suggest that the better performance in stiffness mostly relates to well-interlocked self-assemblies. This may hinder pullout of the clay nanoplatelets as compared to the near perfect layers in LbL assembly. (Differences between LbL-based materials and the nacre-mimetic paper are further discussed in the Supporting Information.) Comparing the various composites with Al_2O_3/chitosan multilayer systems, we can reach higher stiffness values, but cannot yet accomplish the same ductility.[17]

The effect of the different valencies of the counterions and their connectivity on the mechanical properties is remarkable. Increasing the charge of

Table 1: Overview of material characteristics obtained by tensile testing and SAXS for various PDADMAC/MTM nacre papers.

Counterion[a]	Young's modulus E [GPa]	Ultimate stress σ_{UTS} [MPa]	Ultimate strain ε [%]	MTM spacing [nm][b]
Cl^-	12.9 ± 2.8	106 ± 13.7	2.1 ± 0.5	1.86
SO_4^{2-}	24.2 ± 2.7	110 ± 8.7	0.7 ± 0.1	1.85
PO_4^{3-}	32.9 ± 2.2	151 ± 17	0.8 ± 0.1	1.90
$(StSO_3^-)_x$[c]	29.3 ± 2.4	119 ± 8.7	0.6 ± 0.1	2.33
pure[d] PDADMAC	0.16 ± 0.03	12 ± 4	48 ± 9	–

[a] Average of 5–7 samples. [b] Determined from the first-order diffraction peak in SAXS (Supporting Information, Figure S2). The basal spacing of pure MTM is 0.97 nm in the dry state and 1.21 nm in the wet state. [c] Cross-linked. [d] Data for a cast polymer film.[16]

the counterion from monovalent to di- or trivalent leads to a doubling and even tripling of the materials' stiffness. An exchange to the divalent SO_4^{2-} amplifies the Young's modulus to 24 GPa. An increase in charge to the trivalent PO_4^{3-} further fortifies the stiffness to 33 GPa and also the ultimate strength to 151 MPa. The strength already surpasses that of nacre significantly. Clearly, the increasing valence is responsible for a stronger physical cross-linking within the polyelectrolyte layers. In particular, the adhesion between the polycation-coated platelets can be improved, as free ionic groups are located at the outer side of the core/shell building blocks. An increase in mechanical properties can also be achieved by polymerization of the counterions, as in the case of $StSO_3^-$. The connection of the monovalent ions leads to a stiffening of the materials to 29 GPa in Young's modulus and a moderate increase in strength to 119 MPa. Therefore, the preparation of an interpenetrating network of counterions is another efficient means to strengthen the mechanical framework. A main advantage of the ionic cross-linking of the counterions lies in the easy post-processing possibilities.

Therefore, the mechanical performance of our PE-based nacre mimics can be tuned to a large extent by ionic supramolecular interactions. Both the architecture and connectivity of the ions and the charge of the counterions can be used to tailor the mechanical properties. Compared to the efforts that can be spent in tuning the polymer structure, this is a facile approach to improve the mechanics on-demand. It also shows an important design principle for future nacre-mimetic materials using our concept of prefabricated core/shell hard/soft building blocks. Furthermore, considering that the mechanical properties can be altered by thermal polymerization of counterions or possibly by photoinduced valency change,[34–36] these methods can give rise to films with patterned mechanical properties by masked exposures.

Owing to the presence of nitrogen, phosphorus, and chlorine, and a high fraction of clay platelets, we expected an even better fire-resistance and heat-shield capabilities compared to the previously investigated PVA/MTM system,[27] and therefore we explored the properties in more detail. When exposed to high temperature gas flames (ca. 2000 °C), the materials first catch fire for a short moment as the minor-fraction polymer burns off, but immediately self-extinguish upon retraction of the flame. Qualitatively speaking, the materials develop less flames than the PVA/MTM nacre-mimetic paper reported recently, and the flammability decreases in the following order of counterions: $SO_4^{2-} \approx (StSO_3^-)_x > PO_4^{3-} > Cl^-$ (Supporting Information, Video 1). This behavior can be ascribed to the typical fire-retardant effects of the elemental composition. We are convinced that the flammability of the layered composites can be further reduced in future by choosing even better tailored polymers, such as polyphosphazenes. After the intercalated polymer is removed, the materials largely maintain their shape, even for prolonged exposure to the flame.

We also observed excellent flame and heat-shield capabilities once the organic component is removed (Figure 4a; Supporting Information, Video 2). Exposure to a flame causes a bright red glowing spot on the front of the specimens, but much less brightness on the back. This heat insulation originates from the layered micro/nanoporous fully inorganic structure in the center and a fire-protective dense armored skin on the outside (Figure 4c). The formation of the porous structure goes along with a circa fivefold expansion of the thickness of the material during the burning of the intercalated polymer. This response is truly attractive, as it increases the thermal energy dissipation. This promising observation prompted us to demonstrate our nacre mimics for the protection of a flammable biological material. A silk cocoon placed behind a heat shield (initially less than 0.1 mm thick) did not catch fire even upon prolonged exposure (Figure 4b, Supporting Information, Video 3). The composites therefore act as efficient thermal and flame shields similar to ceramics. Interestingly, the material keeps its shape and has a reasonable mechanical stability. Even after the high-temperature treatment, the specimens can be dropped from over 30 cm, and no special care is needed when handling them with tweezers (Supporting Information, Video 4). The condensation of the silanol groups at the clay surfaces fortifies the inorganic network into a stable porous framework with a tightly armored skin where exposed to the flame. Owing to the wavy and more brittle character of the burned specimens, standard tensile testing could not be applied. Preliminary results from nanointendation reveal a complex mechanical behavior due to an oriented multiscale and porous structure, which requires to be studied in a dedicated article. Considering that our approach allows producing these ceramic-like

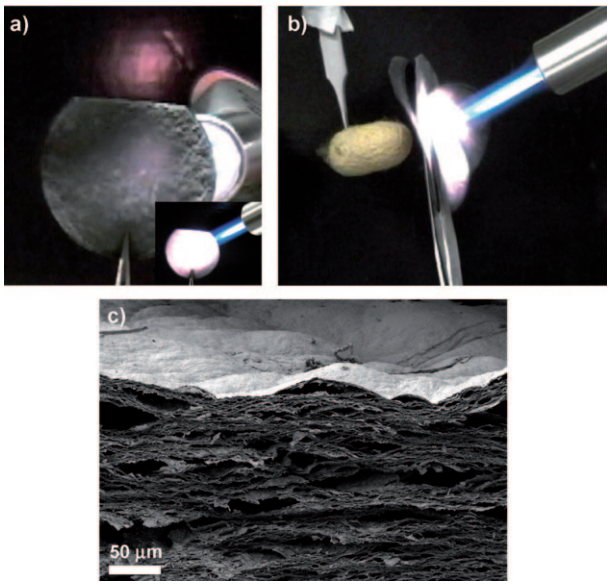

Figure 4. Flame and heat shielding properties of nacre papers. a) Photograph of an initially 0.08 mm thick film exposed to a gas burner from the back side (at ca. 2000 °C) after the polymer is removed. Note the only slight spot at the front of the sample (the bright red spot in the background is a reflection). Inset: a photograph from the other side, showing the exposed surface. b) Nacre-mimetic paper used as a fire and heat shield to protect a silk cocoon positioned about 8 mm behind the shield. (For videos, see the Supporting Information.) c) An SEM image of the nacre paper after flame treatment, showing the development of a tightly armored skin and mesoporous layered interior.

materials from economic starting materials in much more energy-efficient ways than in case of ceramics, we strongly believe that they will be of broad interest as fire-protective films and coatings.

In conclusion, shape-persistent, fire and heat-shielding capabilities together with the lightweight character and the excellent mechanical properties, partly exceeding nacre, are of outmost importance in construction, transportation (air, sea, land, and space) or the defense sector. The elegant control of the supramolecular bonding motifs enables us to tailor and strengthen the mechanical properties on demand and possibly in a patterned fashion. On a short timescale, such properties in combination with simple, rapid, scalable and both economic and green processing strategies can promote sustainability and fully validate the concept of biomimetics for modern materials. We imagine the development of a variety of applications and novel concepts emerging from this attractive strategy toward nacre-mimetic materials.

Received: March 16, 2010
Revised: May 15, 2010
Published online: July 27, 2010

Keywords: biomimetic materials · fire-retardant materials · nacre · self-assembly · supramolecular chemistry

[1] G. Mayer, *Science* **2005**, *310*, 1144.
[2] P. Fratzl, H. S. Gupta, F. D. Fischer, O. Kolednik, *Adv. Mater.* **2007**, *19*, 2657.
[3] M. A. Meyers, P. Y. Chen, A. Y. M. Lin, Y. Seki, *Prog. Mater. Sci.* **2008**, *53*, 1.
[4] M. F. Ashby, L. J. Gibson, U. Wegst, R. Olive, *Proc. R. Soc. London Ser. A* **1995**, *450*, 123.
[5] H. D. Espinosa, J. E. Rim, F. Barthelat, M. J. Buehler, *Prog. Mater. Sci.* **2009**, *54*, 1059.
[6] F. Barthelat, C. M. Li, C. Comi, H. D. Espinosa, *J. Mater. Res.* **2006**, *21*, 1977.
[7] A. P. Jackson, J. F. V. Vincent, R. M. Turner, *Proc. R. Soc. London Ser. B* **1988**, *234*, 415.
[8] R. Z. Wang, Z. Suo, A. G. Evans, N. Yao, I. A. Aksay, *J. Mater. Res.* **2001**, *16*, 2485.
[9] P. Podsiadlo, A. K. Kaushik, B. S. Shim, A. Agarwal, Z. Tang, A. M. Waas, E. M. Arruda, N. A. Kotov, *J. Phys. Chem. B* **2008**, *112*, 14359.
[10] S. M. Lee, E. Pippel, U. Gosele, C. Dresbach, Y. Qin, C. V. Chandran, T. Brauniger, G. Hause, M. Knez, *Science* **2009**, *324*, 488.
[11] S. Pavlidou, C. D. Papaspyrides, *Prog. Polym. Sci.* **2008**, *33*, 1119.
[12] M. A. Hartmann, P. Fratzl, *Nano Lett.* **2009**, *9*, 3603.
[13] P. Podsiadlo, A. K. Kaushik, E. M. Arruda, A. M. Waas, B. S. Shim, J. Xu, H. Nandivada, B. G. Pumplin, J. Lahann, A. Ramamoorthy, N. A. Kotov, *Science* **2007**, *318*, 80.
[14] P. Podsiadlo, M. Michel, K. Critchley, S. Srivastava, M. Qin, J. W. Lee, E. Verploegen, A. J. Hart, Y. Qi, N. A. Kotov, *Angew. Chem.* **2009**, *121*, 7207; *Angew. Chem. Int. Ed.* **2009**, *48*, 7073.
[15] P. Podsiadlo, B. S. Shim, N. A. Kotov, *Coord. Chem. Rev.* **2009**, *253*, 2835.
[16] P. Podsiadlo, M. Michel, J. Lee, E. Verploegen, N. W. S. Kam, V. Ball, J. Lee, Y. Qi, A. J. Hart, P. T. Hammond, N. A. Kotov, *Nano Lett.* **2008**, *8*, 1762.
[17] L. J. Bonderer, A. R. Studart, L. J. Gauckler, *Science* **2008**, *319*, 1069.
[18] E. Munch, M. E. Launey, D. H. Alsem, E. Saiz, A. P. Tomsia, R. O. Ritchie, *Science* **2008**, *322*, 1516.
[19] S. Deville, E. Saiz, R. K. Nalla, A. P. Tomsia, *Science* **2006**, *311*, 515.
[20] M. M. Malwitz, A. Dundigalla, V. Ferreiro, P. D. Butler, M. C. Henk, G. Schmidt, *Phys. Chem. Chem. Phys.* **2004**, *6*, 2977.
[21] T. Ebina, F. Mizukami, *Adv. Mater.* **2007**, *19*, 2450.
[22] H. Tetsuka, T. Ebina, H. Nanjo, F. Mizukami, *J. Mater. Chem.* **2007**, *17*, 3545.
[23] B. R. Heywood, S. Mann, *Adv. Mater.* **1994**, *6*, 9.
[24] A. Sellinger, P. M. Weiss, A. Nguyen, Y. F. Lu, R. A. Assink, W. L. Gong, C. J. Brinker, *Nature* **1998**, *394*, 256.
[25] T.-H. Lin, W.-H. Huang, I.-K. Jun, P. Jiang, *Chem. Mater.* **2009**, *21*, 2039.
[26] G. Decher, *Science* **1997**, *277*, 1232.
[27] A. Walther, I. Bjurhager, J.-M. Malho, J. Pere, J. Ruokolainen, L. Berglund, O. Ikkala, *Nano Lett.* **2010**. DOI: 10.1021/nl1003224.
[28] A. V. Dobrynin, *Curr. Opin. Colloid Interface Sci.* **2008**, *13*, 376.
[29] P. Grochowski, J. Trylska, *Biopolymers* **2008**, *89*, 93.
[30] M. Ballauff, *Prog. Polym. Sci.* **2007**, *32*, 1135.
[31] A. V. Dobrynin, M. Rubinstein, *Prog. Polym. Sci.* **2005**, *30*, 1049.
[32] G. S. Manning, J. Ray, *J. Biomol. Struct. Dyn.* **1998**, *16*, 461.
[33] G. Odian, *Principles of Polymerization*, 4th ed., Wiley, New York, **2004**.
[34] F. A. Plamper, J. R. McKee, A. Laukkanen, A. Nykanen, A. Walther, J. Ruokolainen, V. Aseyev, H. Tenhu, *Soft Matter* **2009**, *5*, 1812.
[35] F. A. Plamper, A. Walther, A. H. E. Mueller, M. Ballauff, *Nano Lett.* **2007**, *7*, 167.
[36] F. A. Plamper, L. Murtomaki, A. Walther, K. Kontturi, H. Tenhu, *Macromolecules* **2009**, *42*, 7254.

